Available online at www.sciencedirect.com

ScienceDirect

International Journal of Solids and Structures 44 (2007) 6678–6700

INTERNATIONAL JOURNAL OF SOLIDS AND STRUCTURES

www.elsevier.com/locate/ijsolstr

Dynamic response of doubly-curved anisotropic sandwich panels impacted by blast loadings

Terry Hause [a,*], Liviu Librescu [b]

[a] *Department of Mechanical and Civil Engineering, Minnesota State University, Mankato, MN 56001, USA*
[b] *Department of Engineering Science and Mechanics, Virginia Tech, Blacksburg, VA 24061, USA*

Received 19 September 2006; received in revised form 2 March 2007
Available online 12 March 2007

Abstract

Problems related with the modeling and dynamic response to blast loadings of doubly-curved sandwich panels with laminated face sheets are developed. In this respect, the implications of the panel curvature, of anisotropy and stacking sequence of face sheets, of transverse orthotropy of the core, and of structural damping on dynamic response to time-dependent loads are highlighted. As concerns the blast pulses considered in this analysis, these are related to in-air explosions or of traveling shock-waves. Other parameters, mainly geometrical, are also considered in the numerical simulations, and their implications on the dynamic response are put into evidence. Due to the absence of similar results in the specialized literature, this paper is likely to fill a gap in the state of the art of this problem, and provide pertinent results that are instrumental in the design of advanced sandwich shells operating in a dynamic environment. Moreover, the closed-form solutions developed in the paper, can serve as excellent references for comparison with numerical based solutions.

Keywords: Sandwich curved panel; Anisotropic face sheets; Dynamic response; Sonic-boom; Blast load; Traveling shock wave

1. Introduction

A continuous interest for an extensive use of sandwich structures in the construction of advanced supersonic/hypersonic flight vehicle and of reusable space transportation systems has been manifested in the last decade, and is more than sure that this trend will continue and intensify in the years ahead. A similar trend is manifested also in the naval constructions and in automotive and civil engineering as well. Some of the underlying reasons and motivation for this interest emerge, among others, from (i) the possibility to integrate the advanced fiber-reinforced composite materials in the face sheets and the core, their use being likely to provide increased bending stiffness with little resultant weight penalty, long fatigue life, and directional properties of face sheets, (ii) possibility to provide thermal and sound insulation characteristics, as well as a smooth aerodynamic surface in a high-speed flow environment, and (iii) improved fatigue performance, superior energy

* Corresponding author. Tel.: +1 248 345 8078.
E-mail addresses: tjcav01@charter.net (T. Hause), librescu@vt.edu (L. Librescu).

0020-7683/$ - see front matter
doi:10.1016/j.ijsolstr.2007.03.006

absorption and extended operational life as compared to stiffened-reinforced structures that are weakened by the appearance of stress concentration. Needless to say, the development of new manufacturing techniques rendering sandwich structures economically feasible, has contributed heavily to the widespread use of such structures in the aerospace industry.

An important issue that should be addressed when dealing with sandwich composite structures used in the design of combat aircraft, of the reusable space vehicle and of naval vessels is related with their dynamic response to time-dependent loads of the blast type. In spite of its enormous practical importance, to the best of authors' knowledge, this problem was considered for flat sandwich structures, only (see e.g. the papers by Librescu et al. (2004, 2006), Hause and Librescu (2005), and Xue and Hutchinson (2004)). The proceedings of the last two international conferences on sandwich structures (Vinson et al., 2003; Thomsen et al., 2005), the monographs (Vinson, 1991; Zenkert, 1995), as well as the survey papers (Noor et al., 1996; Abrate, 1997; Librescu and Hause, 2000; Vinson, 2001; Frostig, 2003; Hohe and Librescu, 2004), reveal in full the absence of such results from the specialized literature.

Also the paper by Vu-Quoc et al. (1997, 2001), devoted to the dynamic modeling of sandwich shells, do not address the related dynamic response problem.

As a matter of fact, even in the context of standard laminated structures, the dynamic response problem was restricted mainly to flat panels (see e.g. Crocker and Hudson, 1969; Rajamani and Prabhakaran, 1980; Dobyns, 1981; Birman and Bert, 1987; Cederbaum et al., 1988, 1989; Librescu and Nosier, 1990; Reddy, 2004).

In this paper, the dynamic response of doubly-curved anisotropic sandwich panels exposed to time-dependent loads generated by an explosive blast, by a sonic-boom, and by tangential travelling waves will be considered, and the implications of a large number of related physical and geometrical parameters will be put into evidence.

However, in order to address this problem and to render the paper reasonably self-contained, as a necessary pre-requisite, the basic equations of the dynamic theory of advanced sandwich curved panels have to be presented.

It should be mentioned that this paper constitutes a generalization for the case of dynamic response of sandwich curved panels of a number of results by the same authors, devoted to static problems (see e.g. Librescu et al. (1997); Hause et al. (1998)).

2. Basic assumptions

The global mid-surface of the sandwich structure σ, selected to coincide with that of the core layer, is referred to a curvilinear and orthogonal Gaussian coordinate system x_α ($\alpha = 1, 2$), while the thickness coordinate x_3 is considered positive when measured in the direction of the inward normal (see Fig. 1).

The uniform thickness of the core is $2\overline{h}$, while those of the top and bottom faces are h'' and h', respectively. As a result, $H(\equiv 2\overline{h} + h' + h'')$ is the total thickness of the structure.

For the sake of identification, the quantities affiliated with the core layer will be marked by a superposed bar, while those associated with the lower and upper face by a single and double primes, respectively, placed on the right of the respective quantity.

Toward the foundation of the linearized theory of the doubly-curved sandwich structures, the following assumptions are used: (i) the face sheets are manufactured from orthotropic material layers, the axes of orthotropy of the individual plies being not necessarily coincident with the geometrical axes x_α of the structure, (ii) the material of the core layer features orthotropic properties in the transverse shear direction and, in addition, the thickness of the core layer is assumed to be much larger that those of the face sheets, i.e. $2\overline{h} \gg h', h''$, (iii) the theory involves the case of the *weak core* sandwich structures, (iv) a perfect bonding between the face sheets and between the faces and the core is postulated, (v) the incompressibility in transverse normal direction is adopted in both the core and face sheets, (vi) the principle of shallow shell theory is used, (vii) the case of symmetric sandwich structures is considered, implying that $h' = h'' = h$, while $a' = a'' \equiv a = \overline{h} + h/2$ is the distance between the global mid-surface structure and the mid-surface of the top/bottom face sheets, and finally, and (viii) due to the fact that $h', h'' \ll 2\overline{h}$, the transverse shear effects in the face sheets are discarded.

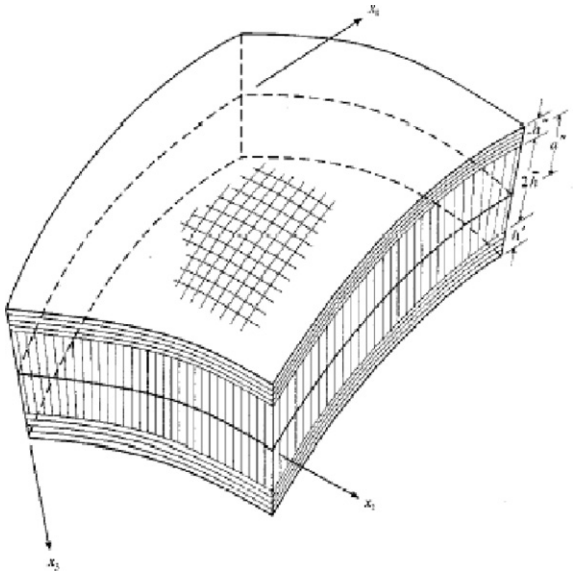

Fig. 1. Geometry of the doubly-curved sandwich panel.

3. Kinematics

3.1. The 3D displacement field in the face sheets and the core

As a result of the previously mentioned assumptions, the 3D distributions of the displacement field fulfilling the kinematic continuity conditions at the interfaces between the core and face sheets (see Librescu (1975); Librescu et al. (1997); Hause et al. (1998)) are represented as:

In the bottom face sheets ($\overline{h} \leqslant x_3 \leqslant \overline{h} + h'$):

$$\left.\begin{aligned} V'_1(x_\alpha, x_3, t) &= \xi_1(x_\alpha, t) + \eta_1(x_\alpha, t) - (x_3 - a)\partial v_3(x_\alpha, t)/\partial x_1, \\ V'_\alpha(x_\alpha, x_3, t) &= \xi_2(x_\alpha, t) + \eta_2(x_\alpha, t) - (x_3 - a)\partial v_3(x_\alpha, t)/\partial x_2, \\ V'_3(x_\alpha, x_3, t) &= v_3(x_\alpha, t). \end{aligned}\right\} \tag{1a–c}$$

In the core ($-\overline{h} \leqslant x_3 \leqslant \overline{h}$):

$$\left.\begin{aligned} \overline{V}_1(x_\alpha, x_3, t) &= \xi_1(x_\alpha, t) + x_3/\overline{h}\left\{\eta_1(x_\alpha, t) + \tfrac{h}{2}\partial v_3(x_\alpha, t)/\partial x_1\right\}, \\ \overline{V}_2(x_\alpha, x_3, t) &= \xi_2(x_\alpha, t) + x_3/\overline{h}\left\{\eta_2(x_\alpha, t) + \tfrac{h}{2}\partial v_3(x_\alpha, t)/\partial x_2\right\}, \\ \overline{V}_3(x_\alpha, x_3, t) &= v_3(x_\alpha, t). \end{aligned}\right\} \tag{2a–c}$$

In the top face sheets ($-\overline{h} - h'' \leqslant x_3 \leqslant -\overline{h}$):

$$\left.\begin{aligned} V''_1(x_\alpha, x_3, t) &= \xi_1(x_\alpha, t) - \eta_1(x_\alpha, t) - (x_3 + a)\partial v_3(x_2, t)/\partial x_1, \\ V''_2(x_\alpha, x_3, t) &= \xi_2(x_\alpha, t) - \eta_2(x_\alpha, t - (x_3 + a)\partial v_3(x_\alpha, t)/\partial x_2, \\ V''_3(x_\alpha, x_3, t) &= v_3(x_\alpha, t) \end{aligned}\right\} \tag{3a–c}$$

In these equations, $V_i(x_\alpha, x_3, t)$ are the 3D displacement components in the direction of the coordinate x_i, while $\xi_\alpha = (V'_\alpha + V''_\alpha)/2$ and $\eta_\alpha = (V'_\alpha - V''_\alpha)/2$ denote the average and half difference of the tangential displacements V'_α and V''_α of the points of the mid-surfaces of the bottom and top face sheets, respectively.

In the previous and the remaining equations, the Greek indices take the values 1 and 2, while the Latin indices have the values 1, 2, and 3, and unless otherwise stated, the Einstein summation convention over the repeated indices is employed.

3.2. Distribution of strain quantities across the shell thickness

In order to obtain the distribution of 2D strain measures across the shell thickness, Eqs. (1)–(3) are used in the 3D strain–displacement relationships expressed as

$$2e_{ij} = V_{i\|j} + V_{j\|i}, \tag{4}$$

where $()_{i\|j}$ denotes 3D the covariant derivative. Employing the relationships between the covariant derivatives of space and surface tensors, (see Librescu, 1975), from Eqs. (1)–(3) in conjunction with Eq. (4) and consistent with the concept of shallow shells one obtains, as part of these equations, the distribution of strain quantities across the shell thickness as well as the expression of 2D strain quantities. While the former item is presented next, the expressions of 2D strain measures are supplied in Appendix A.

Distribution of 3D strains:

In the bottom face sheets $(\overline{h} \leqslant x_3 \leqslant \overline{h} + h')$

$$\begin{aligned} e'_{11} &= \varepsilon'_{11} + (x_3 - a')\kappa'_{11}, \\ e'_{22} &= \varepsilon'_{22} + (x_3 - a')\kappa'_{22}, \\ 2e'_{12} &= \gamma'_{12} + (x_3 - a')\kappa'_{12}. \end{aligned} \tag{5a–c}$$

In the soft core layer $(\overline{h} \leqslant x_3 \leqslant \overline{h})$

$$2\overline{e}_{13} = \overline{\gamma}_{13}, \quad 2\overline{e}_{23} = \overline{\gamma}_{23}, \tag{6a, b}$$

and

In the top face sheets: $(-\overline{h} - h'' \leqslant x_3 \leqslant -\overline{h})$

$$\begin{aligned} e''_{11} &= \varepsilon''_{11} + (x_3 + a'')\kappa''_{11}, \\ e''_{22} &= \varepsilon''_{22} + (x_3 + a'')\kappa''_{22}, \\ 2e''_{12} &= \gamma''_{12} + (x_3 + a'')\kappa''_{12}. \end{aligned} \tag{7a–c}$$

In these equations, the 2D strain measures, ε_{11}, ε_{22}, ε_{12} $(\equiv \gamma_{12}/2)$ denote the tangential strain measures; κ_{11}, κ_{22} and κ_{12} denote the bending strains, while $\overline{\varepsilon}_{13}(\equiv \overline{\gamma}_{13}/2)$, $\overline{\varepsilon}_{23}(\equiv \overline{\gamma}_{23}/2)$ denote the 2D transverse shear strain measures. Their expressions in terms of the 2D displacement measures ξ_1, ξ_2, η_1, η_2 and v_3 are displayed in Appendix A.

4. Governing equations

Hamilton's principle is used to derive the equations of motion and boundary conditions, (see Librescu, 1975).

It is formulated as

$$\delta J = \delta \int_{t_0}^{t_1} (U - W - T)\,\mathrm{d}t = 0, \tag{8}$$

where t_0, and t_1 are two arbitrary instants of time; U denotes the strain energy; W denotes the work done by surface tractions, edge loads and body forces; T denotes the kinetic energy of the 3D body of the sandwich structure, while δ is the variation operator.

In Eq. (8)

$$\delta U = \tfrac{1}{2}\int_{\sigma}\left[\int_{\overline{h}}^{\overline{h}+h'} \sigma'_{ij}\delta e'_{ij} + \int_{-\overline{h}}^{+\overline{h}} \overline{\sigma}_{ij}\delta\overline{e}_{ij} + \int_{-\overline{h}-h''}^{-\overline{h}} \sigma''_{ij}\delta e''_{ij}\right]\mathrm{d}x_3\,\mathrm{d}\sigma \quad (i,j=1,2,3) \tag{9}$$

where σ_{ij} denotes the stress tensor and σ denotes the mid-surface area of the sandwich panel. In addition, as a result of Hamilton's condition, $\delta V_i = 0$ at t_0, t_1 one obtains

$$\int_{t_0}^{t_1} \delta T \, \mathrm{d}t = -\int_{t_0}^{t_1} \mathrm{d}t \left[\int_{\sigma} \int_{\overline{h}}^{\overline{h}+h'} \rho' \ddot{V}'_i \delta V'_i \, \mathrm{d}x_3 + \int_{-\overline{h}}^{\overline{h}} \overline{\rho} \ddot{\overline{V}}_i \delta \overline{V}_i \, \mathrm{d}x_3 + \int_{-\overline{h}-h''}^{-\overline{h}} \rho'' \ddot{V}''_i \delta V''_i \, \mathrm{d}x_3 \right], \tag{10}$$

while the variation of work done by the body forces and external loads is

$$\delta W = \int_{\sigma} \left[\int_{\overline{h}}^{\overline{h}+h'} \rho' H'_i \delta V'_i \, \mathrm{d}\sigma \, \mathrm{d}x_3 + \int_{-\overline{h}}^{\overline{h}} \overline{\rho} \overline{H}_i \delta \overline{V}_i \, \mathrm{d}\sigma \, \mathrm{d}x_3 + \int_{-\overline{h}-h''}^{-\overline{h}} \rho'' H''_i \delta V''_i \, \mathrm{d}\sigma \, \mathrm{d}x_3 \right] + \int_{\Omega_s} \underset{\sim}{\sigma}_i \delta V_i \, \mathrm{d}\Omega. \tag{11}$$

In Eq. (10) the superposed dots denote time derivatives, ρ denotes the mass density of the constituent materials, $\sigma_i = \sigma_{ij} n_j$ denote the components of the stress vector prescribed on the part Ω_σ of the external boundary Ω, n_i are the components of the outward unit vector normal to Ω, while H_i denote the components of the body force vector.

From Eq. (8) considered in conjunction with Eqs. (9)–(11), with the constitutive equations (see Appendix C) and the strain–displacement relationships (used as subsidiary conditions), carrying out the integration with respect to x_3 and integrating by parts whenever feasible; using the expression of global stress resultants and stress couples (to be defined later), by retaining only the transversal load, transversal inertia, and transverse damping, and invoking the arbitrary and independent character of variations $\delta\eta_1$, $\delta\eta_2$, $\delta\eta_1$, $\delta\eta_2$, δv_3 and $\delta v_{3,n}$ throughout the entire domain of the shell and within the time interval $[t_0, t_1]$, the governing equations of motion and the boundary conditions of doubly-curved sandwich shells are derived. By including also the effect of bi-axial edge loads N^0_{11} and N^0_{22} considered to be positive in compression, the obtained governing equations expressed in operatorial form in terms of the 2D displacement measures ξ_1, ξ_2, η_1, η_2 and v_3 are

$$\begin{aligned}
&\mathcal{L}_{11} V_1 + \mathcal{L}_{12} V_2 + \mathcal{L}_{13} V_3 + \mathcal{L}_{14} V_4 + \mathcal{L}_{15} V_5 = 0,\\
&\mathcal{L}_{21} V_1 + \mathcal{L}_{22} V_2 + \mathcal{L}_{23} V_3 + \mathcal{L}_{24} V_4 + \mathcal{L}_{25} V_5 = 0,\\
&\mathcal{L}_{31} V_1 + \mathcal{L}_{32} V_2 + \mathcal{L}_{33} V_3 + \mathcal{L}_{34} V_4 + \mathcal{L}_{35} V_5 = 0,\\
&\mathcal{L}_{41} V_1 + \mathcal{L}_{42} V_2 + \mathcal{L}_{43} V_3 + \mathcal{L}_{44} V_4 + \mathcal{L}_{45} V_5 = 0,\\
&\mathcal{L}_{51} V_1 + \mathcal{L}_{52} V_2 + \mathcal{L}_{53} V_3 + \mathcal{L}_{54} V_4 + \mathcal{L}_{55} V_5 = p_3(x_1, x_2, t),
\end{aligned} \tag{12a–e}$$

where $V_i = \{\xi_1, \xi_2, \eta_1, \eta_2, v_3\}^T$ is the generalized displacement vector, while $\mathcal{L}_{ij} = \mathcal{L}_{ji}$ are 2D partial differential operators. Their expressions are provided in Appendix D.

In compact form, the governing equations system can be expressed as

$$\mathcal{L}_{ij} V_j = \mathcal{F}_i \quad (i, j = \overline{1,5}). \tag{13}$$

As concerns the load terms $\mathcal{F}_i$ appearing in Eq. (15), these are as follows

$$\mathcal{F}_1 = \mathcal{F}_2 = \mathcal{F}_3 = \mathcal{F}_4 = 0 \quad \text{and} \quad \mathcal{F}_5 = p_3(x_1, x_2, t). \tag{14a}$$

In addition,

$$\{d_1, d_2\} = (2\overline{K}^2/\overline{h})\{\overline{G}_{13}, \overline{G}_{23}\}. \tag{14b}$$

The governing equation system (12) consisting of five equations in five displacement quantities is rather general, in the sense that it can address the free vibration and dynamic response problems of large classes of doubly-curved shallow sandwich shells. In particular, the obtained governing system is applicable to circular cylindrical sandwich shells of both closed and open transverse cross-sections.

One should also remark that in the case of flat sandwich panels, implying $1/R_1 = 1/R_2 = 0$, the governing system (12) exactly decouples into two independent systems, one of the fourth order in terms of displacements ξ_1 and ξ_2, associated with the stretching problem, and the other one, of the eighth order, in terms of η_1, η_2 and v_3, governing the bending problem. It should also be remarked that the $|\mathcal{L}_{ij}|$ operator can be seen as the Donnell-Mushtari-Vlasov extension to the case of sandwich shells, of the isotropic (Gol'denveiser, 1961; Leissa, 1973) and laminated shells (Qatu, 2004) counterparts. It should be noticed that the symmetry of the $|\mathcal{L}_{ij}|$ operator precludes the occurrence of complex eigenvalues and ensures the orthogonality of eigenfunctions (Librescu, 1975).

5. Blast loads

The structure of combat aircraft or of space vehicles can be exposed during their operational life to blast pulses generated by an explosion, or by shock-wave disturbances produced by an aircraft flying at supersonic speeds, or by any supersonic projectile, rocket or missile operating in its vicinity.

In the latter case, the blast pulse is referred to as sonic-boom. Its time-history is described as an N-shape pulse, featuring both a positive and a negative phase. Having in view the large blast front generated by the explosion as compared to the relatively small dimensions of the panel, one assumes with sufficient accuracy that the pressure is uniform over the entire panel that is impacted at normal incidence.

The sonic-boom overpressure can be expressed as follows (see e.g. Librescu and Nosier, 1990),

$$p_3(t) = \begin{cases} P_0(1 - t/t_p) & \text{for } 0 < t < rt_p, \\ 0 & \text{for } t < 0 \text{ and } t > rt_p, \end{cases} \tag{15}$$

where P_0 denotes the peak reflected pressure in excess to the ambient one, t_p denotes the positive phase duration of the pulse measured from the time of impact of the structure, and r denotes the shock pulse length factor.

For $r = 1$, the sonic-boom degenerates into a triangular explosive pulse, for $r = 2$, a symmetric sonic-boom pulse is obtained while $r \neq 2$ corresponds to a nonsymmetric N-pulse. When $r = 1$ and $t_p \to \infty$, in Eq. (15) the N-pulse degenerates in a step pulse.

A more complete expression of the explosive blast pulse as compared to the triangular one is described by Friedländer exponential decay equation as

$$p_3(t) = P_0\left(1 - \frac{t}{t_p}\right)e^{-a't/t_p}, \tag{16}$$

where the negative phase of the blast is included. In Eq. (16) a' denotes a decay parameter which has to be adjusted to approximate the pressure curve from the blast test. As it could be inferred, the triangular explosive load may be viewed as a limiting case of Eq. (16), that is for $a'/t_p \to 0$.

Having in view that Laplace transform method will be used to determine the dynamic response, it is appropriate to express Eq. (15) equivalently (see Marzocca et al., 2001), as

$$p_3(t) = P_0\left(1 - \frac{t}{t_p}\right)[H(t) - H(t - rt_p)], \tag{17}$$

where $H(t)$ denotes the Heaviside step function.

As special cases of Eq. (17), the rectangular and step pressure pulses can be obtained. In the former case

$$p_3(t) = P_0\{H(t) - H(t - t_p)\}, \tag{18a}$$

while for the latter one

$$p_3(t) = P_0 \quad \text{for } \forall t > 0. \tag{18b}$$

The sine pulse that will also be considered in the numerical simulations, is represented as

$$p_3(t) = \begin{cases} P_0 \sin \pi t/t_p, & 0 \leqslant t \leqslant t_p, \\ 0, & t > t_p. \end{cases} \tag{19}$$

Finally, in the case of an air-blast traveling in the tangential direction to the panel span, case that will also be considered, the pressure time-history is represented as

$$p_3(t) = P_0 e^{-\eta(ct - x_1)}H(ct - x_1), \tag{20}$$

where c is the wave speed in the medium surrounding the structure, while η is an exponent determining the character of the blast decay.

For a recent study regarding the modeling of gun blast pressure pulses, the reader is referred to Kim and Han (2006).

6. Solution methodology

The solution methodology developed by Librescu et al. (1997) and Hause et al. (1998, 2000) to address static problems of simply supported sandwich shells will be extended to that of the dynamic response.

A cursory examination of Eqs. (12) enables one to remark that with the exception of the last equation that is nonhomogeneous, the first four ones are homogeneous. This feature is very important in the solution procedure that will be adopted here. Considering a doubly-curved panel of rectangular projection ($L_1 \times L_2$) on the horizontal plane for simply supported edges, freely movable in the normal and tangential directions, the boundary conditions are as follows:

at $x_1 = 0,\ L_1$:

$$N_{11} = 0;\ N_{12} = 0,\ \eta_1 = 0,\ \eta_2 = 0,\ M_{11} = 0,\ v_3 = 0, \tag{21a–f}$$

and at $x_2 = 0,\ L_2$:

$$N_{22} = 0,\ N_{12} = 0,\ \eta_1 = 0,\ \eta_2 = 0,\ M_{22} = 0,\ v_3 = 0. \tag{21g–l}$$

In terms of displacement quantities, the first, second and fifth boundary conditions write as:

$$\begin{aligned} &N_{11} \equiv A_{11}\xi_{1,1} + A_{12}\xi_{2,2} + A_{16}(\xi_{2,1} + \xi_{2,2}) - (A_{11}/R_1 + A_{12}/R_2)v_3 = 0 \ (1 \rightleftarrows 2),\\ &N_{12} \equiv A_{66}(\xi_{2,1} + \xi_{1,2}) + A_{26}\xi_{2,2} + A_{16}\xi_{1,1} - (A_{16}/R_1 + A_{26}/R_2)v_3 = 0,\\ &M_{11} \equiv F_{11}v_{3,11} + F_{12}v_{3,22} + 2F_{16}v_{3,12} = 0,\\ &M_{22} \equiv F_{22}v_{3,22} + F_{12}v_{3,11} + 2F_{26}v_{3,12} = 0. \end{aligned} \tag{22a–d}$$

In these equations as well as in the coefficients of governing equations, the global stiffness quantities are defined in Appendix D.

The sign $(1 \rightleftarrows 2)$ accompanying Eq. (22a) indicates that the expressions not explicitly supplied can be obtained from the respective equation upon replacing subscript 1 by 2 and vice-versa. The same convention is used throughout the paper.

In this context, the displacements $\xi_1(x_1, x_2, t)$ $\xi_2(x_1, x_2, t)$ and $v_3(\xi_1, \xi_2, t)$ are represented as

$$\begin{Bmatrix} \xi_1(x_1, x_2, t) \\ \xi_2(x_1, x_2, t) \end{Bmatrix} = \begin{bmatrix} (F_1)_{mn} & (F_2)_{mm} \\ (G_1)_{mn} & (G_2)_{mn} \end{bmatrix} \begin{Bmatrix} \cos\lambda_m x_1 & \sin\mu_n x_2 \\ \sin\lambda_m x_1 & \cos\mu_n x_2 \end{Bmatrix} q_{mn}(t), \tag{23a}$$

$$v_3(x_1, x_2, t) = q_{mn}(t)\sin\lambda_m x_1 \sin\mu_n x_2, \tag{23b}$$

where $(F_i)_{mn}$ $(G_i)_{mn}$ are arbitrary constants to be determined later, while $\lambda_m \equiv m\pi/L_1$ and $\mu_n \equiv n\pi/L_2$, $q_{mn}(t)$ being the generalized coordinates. Using in the same equations the representation of ξ_1 and ξ_2 given by Eq. (23), keeping in mind that in these equations the operators $\mathcal{L}_{\alpha 3}$ and $\mathcal{L}_{\alpha 4}$ are zero, and identifying the coefficients of the same trigonometric functions, one determine F_{mn} and G_{mn} that are supplied in Appendix D.

Based on above representations, Eqs. (12a,b) are identically fulfilled. A procedure aimed at determining $\eta_1(x_1, x_2, t)$ and $\eta_2(x_1, x_2, t)$, similar to that used to determine ξ_1 and ξ_2, is applied to Eqs. (12c,d). To this end, one represent η_1 and η_2 as

$$\begin{Bmatrix} \eta_1(x_1, x_2, t) \\ \eta_2(x_1, x_2, t) \end{Bmatrix} = \begin{bmatrix} (H_1)_{mn} & (H_2)_{mm} \\ (I_1)_{mn} & (I_2)_{mn} \end{bmatrix} \begin{Bmatrix} \cos\lambda_m x_1 & \sin\mu_n x_2 \\ \sin\lambda_m x_1 & \cos\mu_n x_2 \end{Bmatrix} q_{mn}(t), \tag{24}$$

where $(H_i)_{mn}$ and $(I_i)_{mn}$ are undetermined coefficients. Use of representations (20) and (21) in Eqs. (12c,d), followed by the identification of the coefficients of the same trigonometric functions, yields the unknown coefficients that are provided in Appendix E.

In this way, the equations of motion (12a–d) and the boundary conditions (21e–f) and (21k,l) are identically fulfilled. The remaining equation that was not fulfilled is Eq. (12e). This equation as well as the boundary conditions that are not fulfilled, will be satisfied in the Extended Galerkin sense (see Librescu et al., 1997; Hause et al., 1998, 2000).

To this end, one inserts in Hamilton's principle, Eq. (8), the representations of displacement quantities, (23)–(24), carry out the indicated operations, and bearing in mind that the first four equations of equilibrium as well as the geometric boundary conditions are identically fulfilled, one obtains for $q_{mn}(t)$ the equation

$$\ddot{q}_{mn} + 2\Delta_{mn}\omega_{mn}\dot{q}_{mn} + \omega_{mn}^2 q_{mn} = F_{mn}(t). \tag{25}$$

In Eq. (25), $\Delta_{mn} = C/(2m_0\omega_{mn})$ denotes the modal damping factor; while ω_{mn}^2 denotes the undamped eigenfrequencies, their expression being provided in Appendix E, while the generalized load is expressed as

$$F_{mn}(t) = \frac{16\delta_{m,2s-1}\delta_{n,2q-1}}{m_0(2s-1)(2q-1)\pi^2}p_3(t), \tag{26a}$$

where

$$\delta_{m,2s-1} = \begin{cases} 1, & m \text{ odd} \quad (s = 1, 2, \ldots), \\ 0, & m \text{ even}, \end{cases} \tag{26b}$$

the same definition being valid also for $\delta_{n,2q-1}$.

The solution of Eq. (25) for various blast loads was obtained via the unilateral Laplace's transform technique, and in this context, zero initial conditions, implying $q_{mn}(0) = \dot{q}_{mn}(0)$, have been considered. The solution $q_{mn}(t)$ for various pressure pulses is provided in Appendix F.

7. Numerical simulations and discussion

Unless otherwise specified, the numerical simulations are carried out by considering the architecture of the sandwich panel as $[\theta/-\theta/\theta/\text{core}/\theta/-\theta/\theta]$, where θ denotes the ply-angle in the various face sheet layers, θ being positive when measured from the positive x_1-axis toward the positive x_2-axis.

Moreover, the material properties on which bases the results will be generated, are listed in Table 1.

In addition, the doubly-curved sandwich panel is considered to have a square projection on a plane, implying $\phi(=L_1/L_2) = 1$, where $L_1 = 0.420$ m and that $h' = h'' = h = 0.0015$ m and $2\overline{h} = 0.0250$ m. Moreover, unless otherwise stated, $\psi_1(=1/R_1) = \psi_2(=1/R_2) = 0.4$, and $P_0 = 1.38$ MPa. In all numerical simulations, the dimensionless deflection time-history (w/H) for various pressure pulses has been depicted, where $w(\equiv v_3(L_1/2, L_2/2))$ denotes the panel central deflection.

Also, in all supplied figures, there are, as insets, graphical representations of the involved blast pulses, and there is also indicated the stacking-sequence architecture of the panel.

In Figs. 2–5, the effects of various parameters on deflection time-history of central point of sandwich panels subjected to a traveling shock-wave, depicted in the insets of the figures, are presented.

In Fig. 2, the implications of the curvature ratio (L_α/R_α) on the dynamic response have been highlighted. It is clearly seen that for the considered spherical cap the increase of the curvature plays a highly beneficial role toward damping out the oscillations.

In Fig. 3, the effect of the speed of wave propagation, c, was put into evidence. The depicted results reveal that the increase of c yields a rather rapid decay of response amplitudes.

In Fig. 4, there are shown the effects of the ply-angle of face sheets. The results reveal that within the considered stacking sequence, $\theta = 45°$. constitutes the best ply-angle from the dynamic response point of view, in the sense of a rapid decay of the oscillation amplitudes.

Table 1
Material properties of face sheets and core

Face sheets			
E_1 (GPa)	E_2 (GPa)	G_{12} (GPa)	ρ (kg/m^3)
207	5.17	2.55	1588.22
Core layer			
$\overline{G}_{13}$ (GPa)	$\overline{G}_{23}$ (GPa)		$\overline{\rho}$ (kg/m^3)
0.1027	0.0621		16

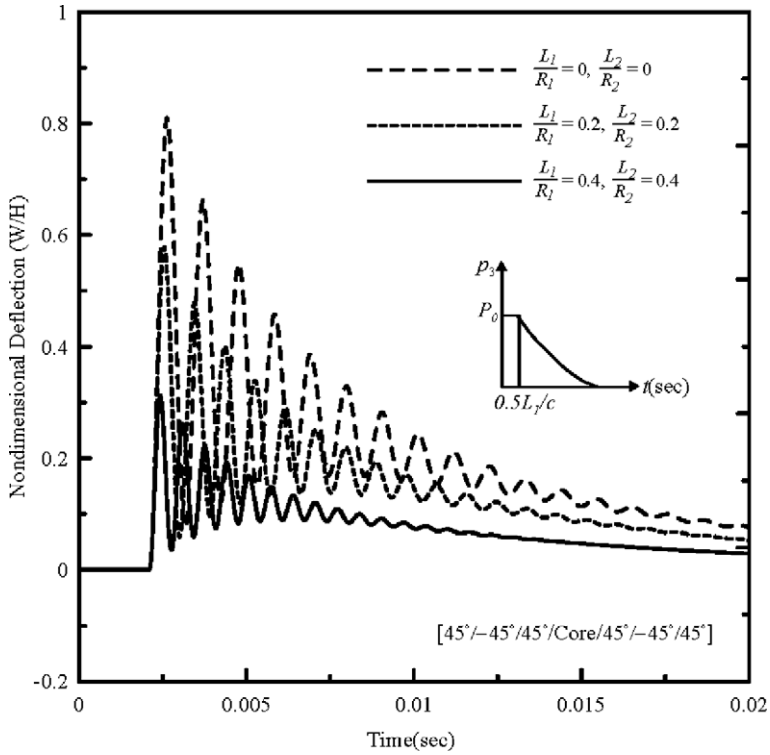

Fig. 2. Implications of the curvature on the dynamic response of normalized deflection amplitude of the panel center. The traveling wave and the panel stacking sequence are depicted in the inset ($c = 100$ m/s).

In Fig. 5, the implications of tangential edge load $K_x(= N_{11}^0 L_1^2/(\pi^4 F_{11}))$ on dynamic response are presented. The results reveal the beneficial effect of tensile edge loads and the detrimental one of the compressive ones.

In Figs. 6–8, the effects generated by a sonic-boom on the panel responses are presented. Particularly, in Fig. 6, for this case the implications of the curvature ratio are put into evidence.

As it clearly appears, the curved panel behaves much better, from the dynamic response point of view, than its flat panel counterpart, in both the forced and free motions. Related with the implications of the ply-angle, Fig. 7 shows a similar trend as in Fig. 4, namely that for the considered panel stacking-sequence, the ply-angle $\theta = 45°$. yields the most rapid decay of the oscillation amplitudes. Fig. 8 presents the effect played by the damping ratio Δ on dynamic response.

The results reveal that the response is extremely sensitive to the damping Δ, and its increase yields a dramatic decrease of oscillation amplitudes in both the free ($rt_p < 0.01$ s) and forced ($rt_p > 0.01$ s), motion ranges.

In Fig. 9, a comparison of the effects generated by three different blast pulses is presented, namely of a traveling shock-wave (tangential blast), of a triangular explosive blast, and of a symmetric ($r = 2$) sonic-boom.

The results reveal that among these three pressure pulses, the sonic-boom results in the most severe response. However, as time-unfolds, the oscillations damp out, and the differences between the responses due to the explosive blast and sonic-boom become immaterial.

In Figs. 10 and 11, the effects of the step pulse considered in conjunction with the ply-angle (Fig. 10) and with that of the curvature ratio (Fig. 11) are presented.

While the results show similar trends as compared to their counterparts obtained for other pressure pulses, they also reveal the severe effects of the structure, in the sense that, even after damping out of oscillations, the structure will experience a uniform deflection that will highly different for various ply-angles and curvature ratios.

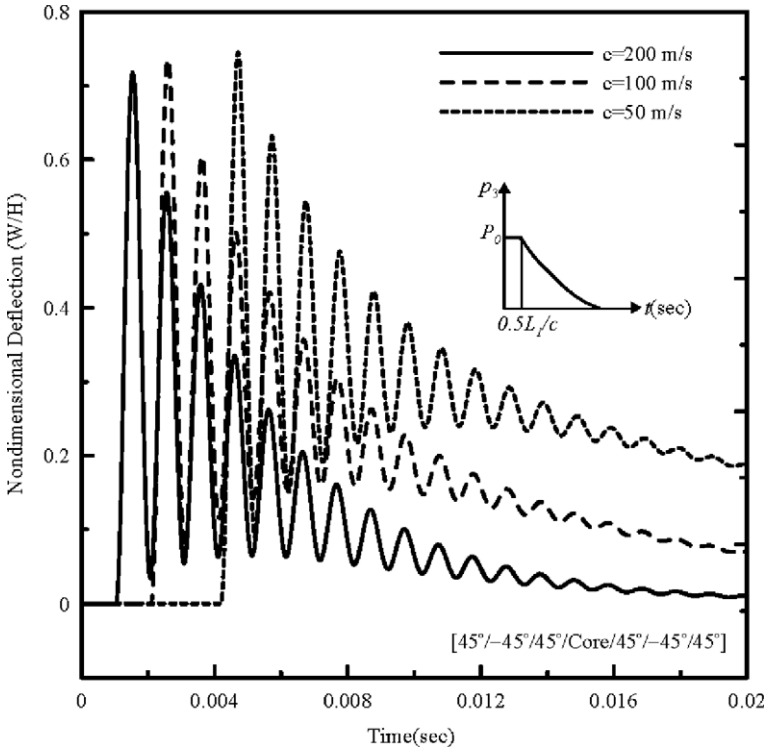

Fig. 3. Implication of the velocity of propagation of the traveling wave on dynamic response ($L_1/R_1 = L_2/R_2 = 0.1$).

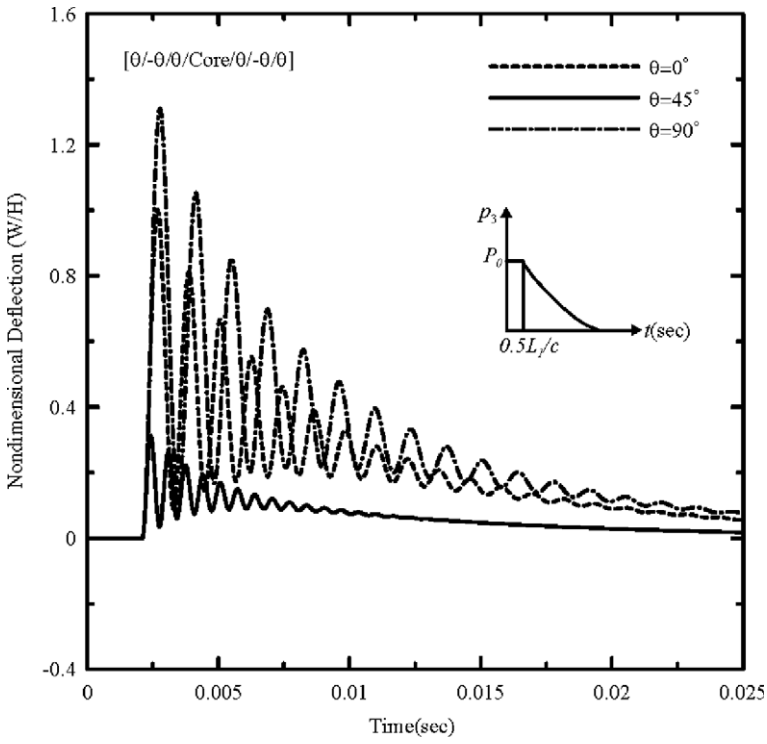

Fig. 4. Implication of ply-angle of face sheets on the dynamic response to traveling waves ($c = 100$ m/s, $L_1/R_1 = R_2/R_2 = 0.4$).

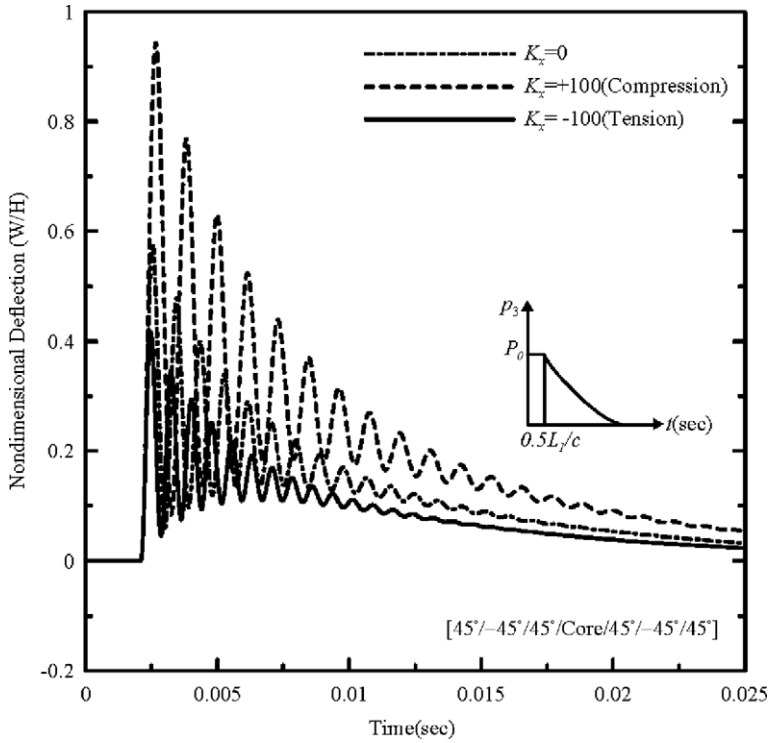

Fig. 5. Effects of tensile/compressive edge loads $K_x(=N_{11}^0 L_1^2/\pi^4 F_{11})$, on dynamic response to traveling waves of a circular cylindrical panel ($c = 100$ m/s, $L_1/R_1 = 0$, $L_2/R_2 = 0.4$).

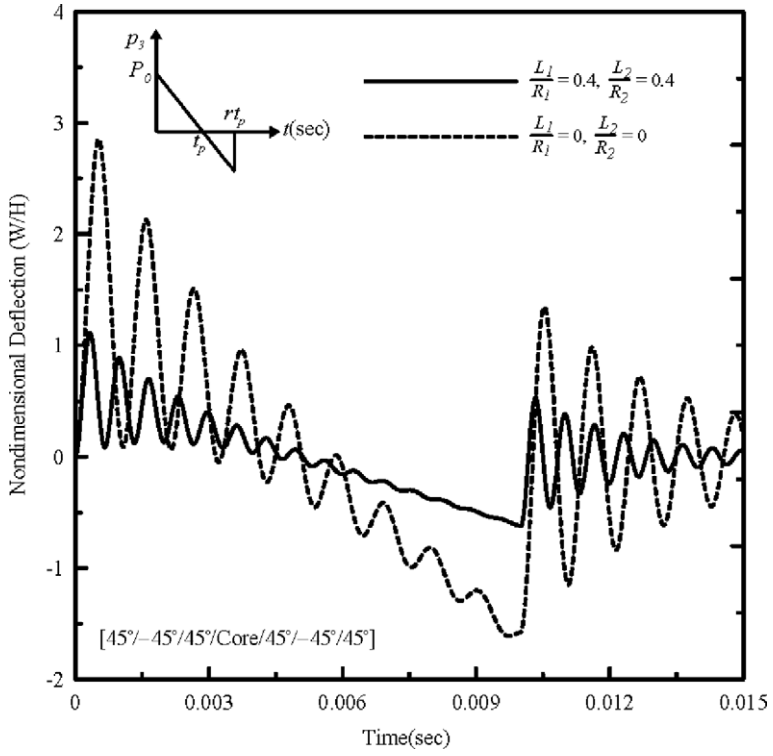

Fig. 6. Dynamic response to a sonic-boom. Implications of the panel curvature ($r = 2$, $t_p = 0.005$ s, $P_0 = 5$ MPa).

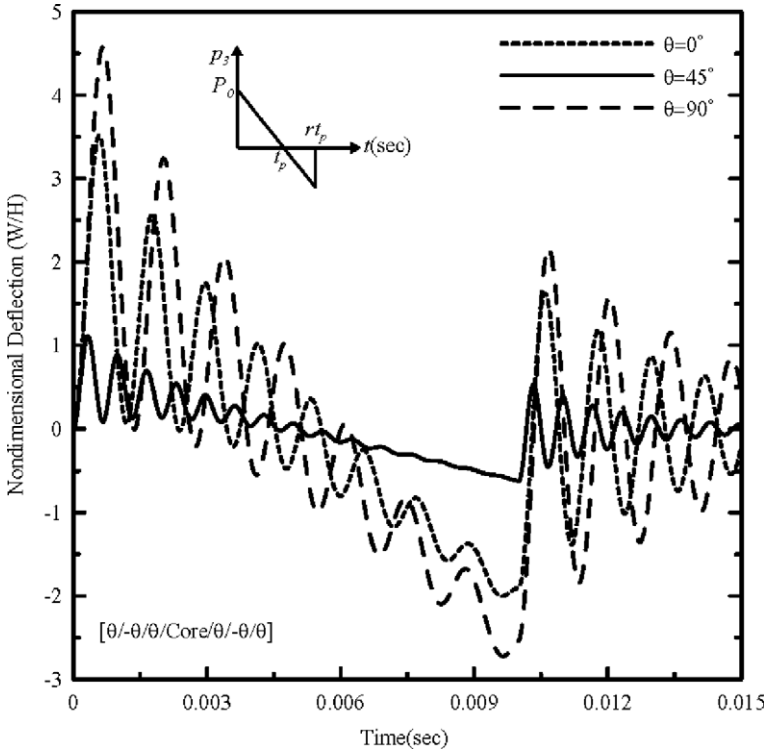

Fig. 7. Implications of ply-angle of face sheets on dynamic response to a sonic-boom. The characteristics of the sonic-boom pressure pulse are as in Fig. 6.

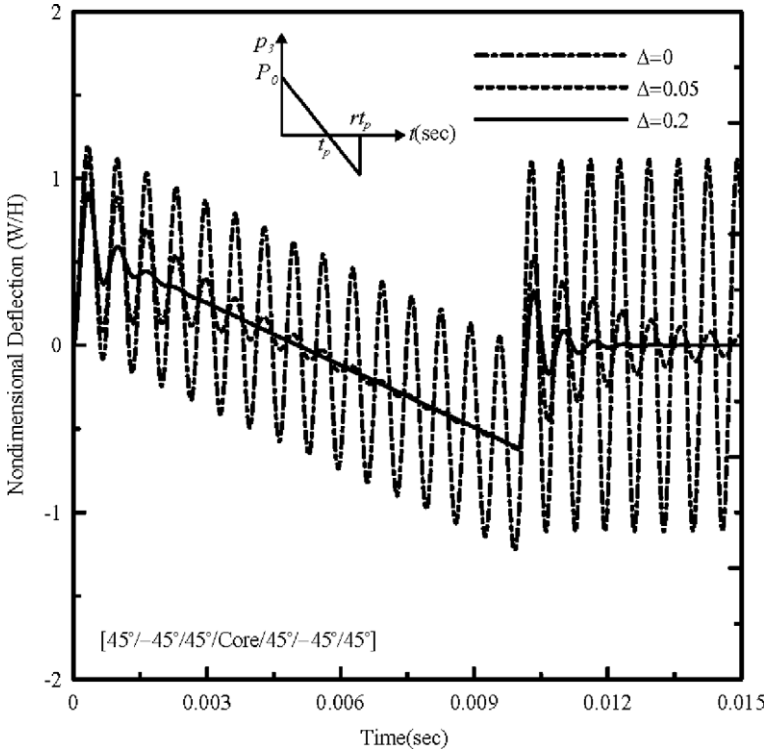

Fig. 8. Implications of structural damping on dynamic response to a sonic-boom pulse. The characteristics of the pulse are as in Fig. 6.

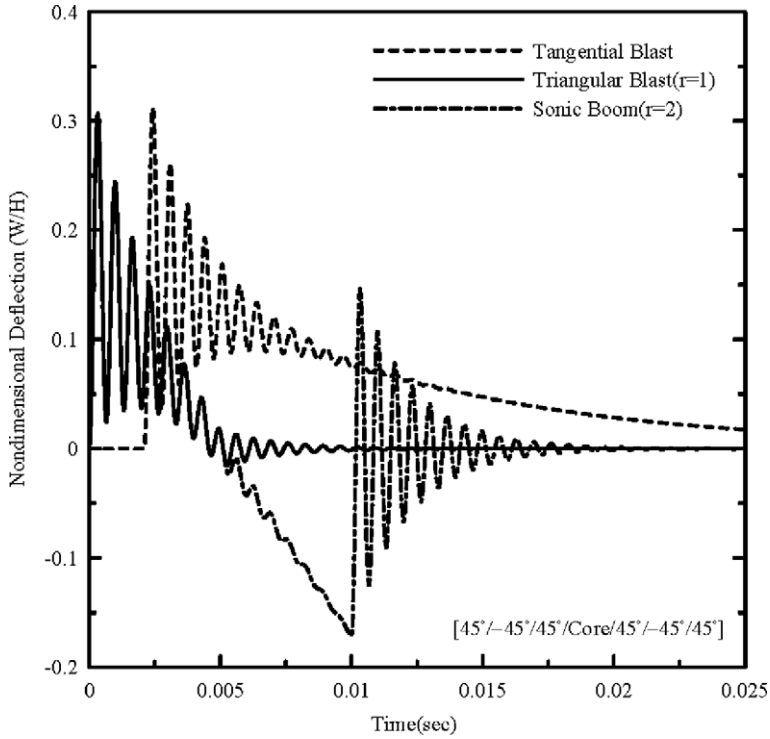

Fig. 9. Implications on dynamic response of various blasts impacting the sandwich panel ($c = 100$ m/s, $P_0 = 1.38$ MPa).

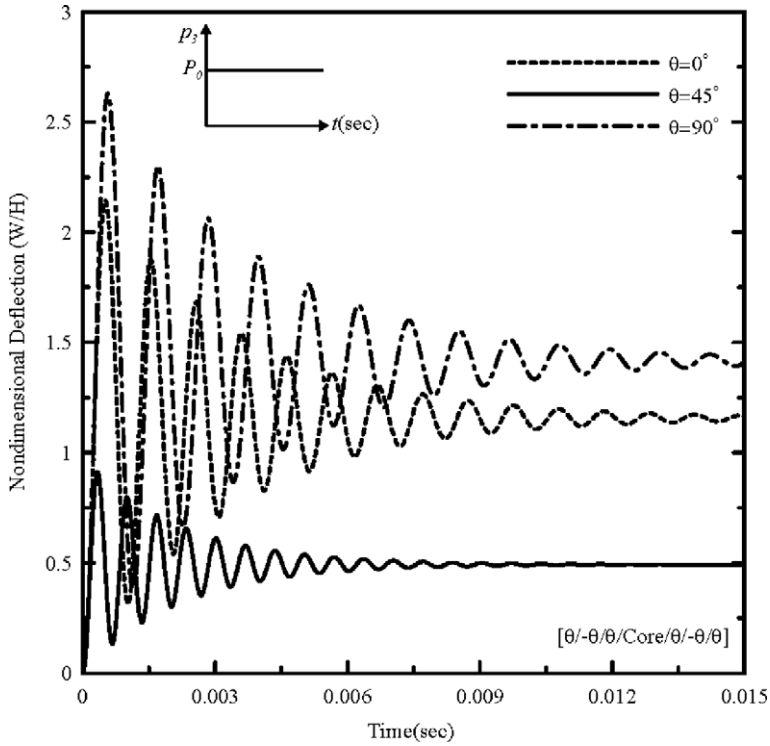

Fig. 10. Implications of the ply-angle of face sheets on the dynamic response to a step pulse ($P_0 = 1.38$ MPa, $\Delta = 0.5$).

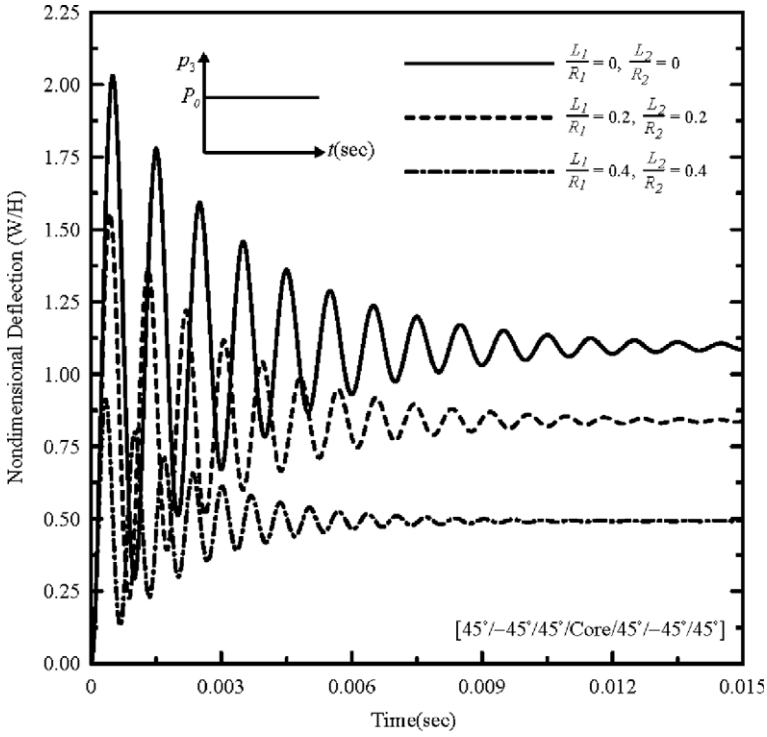

Fig. 11. Influence of panel curvature ratio on dimensionless central deflection time-history of the sandwich panel to a step pulse.

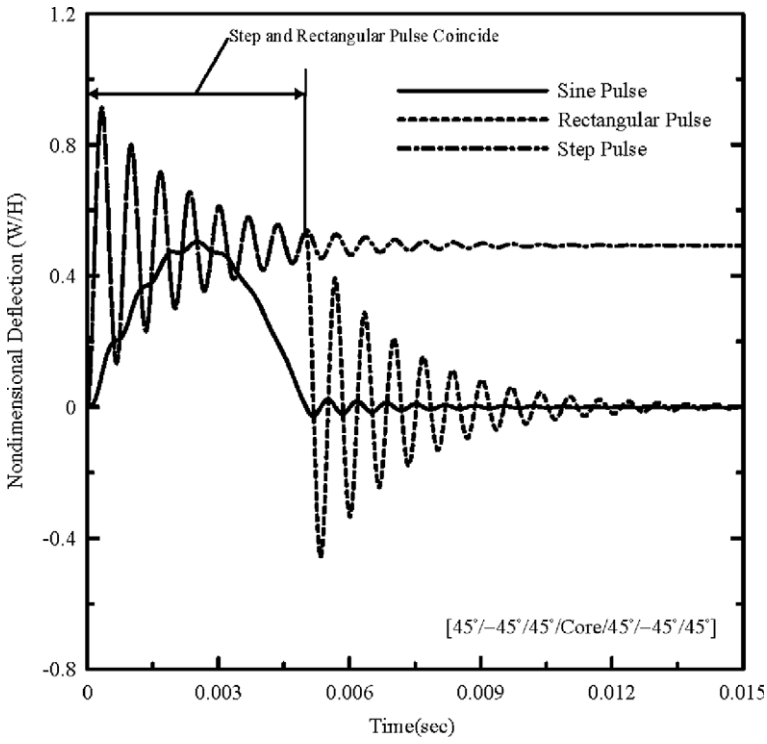

Fig. 12. Comparison of various pressure pulses (sine, rectangular and step) on transversal deflection time-history ($1/R_1 = 1/R_2 = 0.4$).

In Fig. 12 a comparison of the implications of three pressure pulses on dynamic response of sandwich panels is presented. The results reveal that in the forced motion regime, that is for $t < t_p(=0.005\ \text{s})$, the step and the rectangular pulses yields the same deflection amplitude. However, as it becomes apparent, beyond t_p, sharp differences between their responses are experienced. In contrast to their effects, the half-sine pulse yields a significant increase of the deflection amplitude in the forced motion range, that is followed in the free motion range by mild oscillations. However, as it appears from Figs. 13 and 14, the deflection amplitudes can be much larger for the structures featuring lower curvature ratios, or of those for which, the ply-angle is not selected as to provide the maximum bending stiffness, in the present case, $\theta = 45°$.

In Figs. 15 and 16, the response to an explosive blast based on Friendländer's exponential decay pressure model was presented. As it can be seen from these two figures, the panel curvature and the ply-angle constitute very important parameters toward reducing the oscillation amplitudes in both the forced and free motion regimes. Although the numerical simulations have considered only the transversal deflection time-history, based on the expressions of $q_{mn}(t)$ obtained for various pressure pulses and of Eqs. (25a) and (26), one can determine also the dynamic response related with the displacement ξ_α and η_α, and using the appropriate equations, part of them displayed in the paper, one can obtain the time-history for the stress and strain quantities, in various points of the structure. This item is of considerable importance in the studies of damage and failure predictions of sandwich constructions.

It should be indicated here that in the papers by Hohe and Librescu (2004) and Hohe et al. (2006), an encompassing geometrically nonlinear theory of sandwich shells/plates was developed, in which framework the effect related to the compressibility of the core layer was incorporated. Such a structural model enables one to capture, in addition to the global response, also the wrinkling response. When the geometrical nonlinearities are discarded, that sandwich model reduces to that presented in this paper, and in such a context, the response to external time-dependent loads corresponds to the global response only.

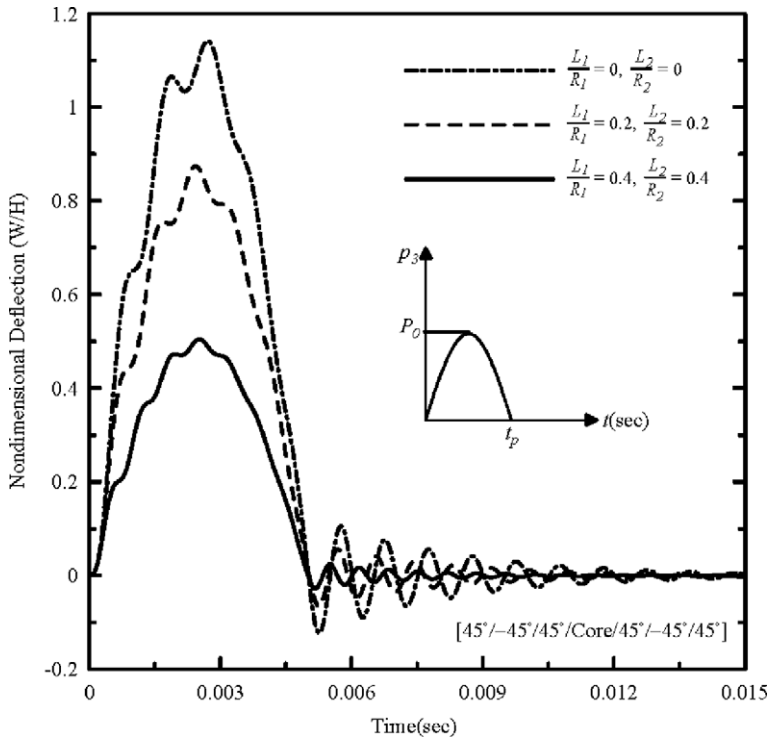

Fig. 13. Implication of curvature ratio on dynamic response of a sandwich panel to a half-sine pressure pulse.

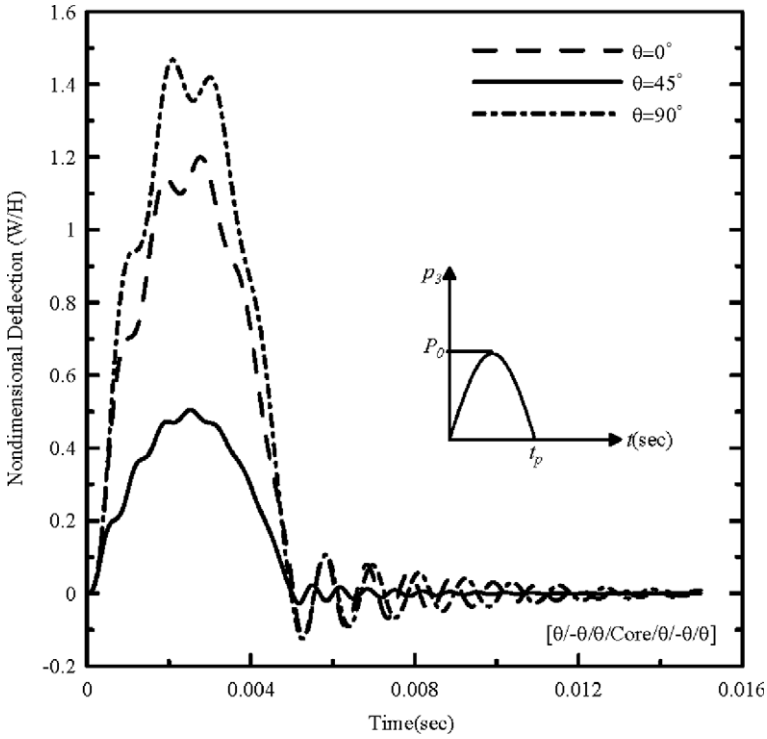

Fig. 14. Influence of the ply-angle of face sheets on dynamic response to a half-sine pressure pulse.

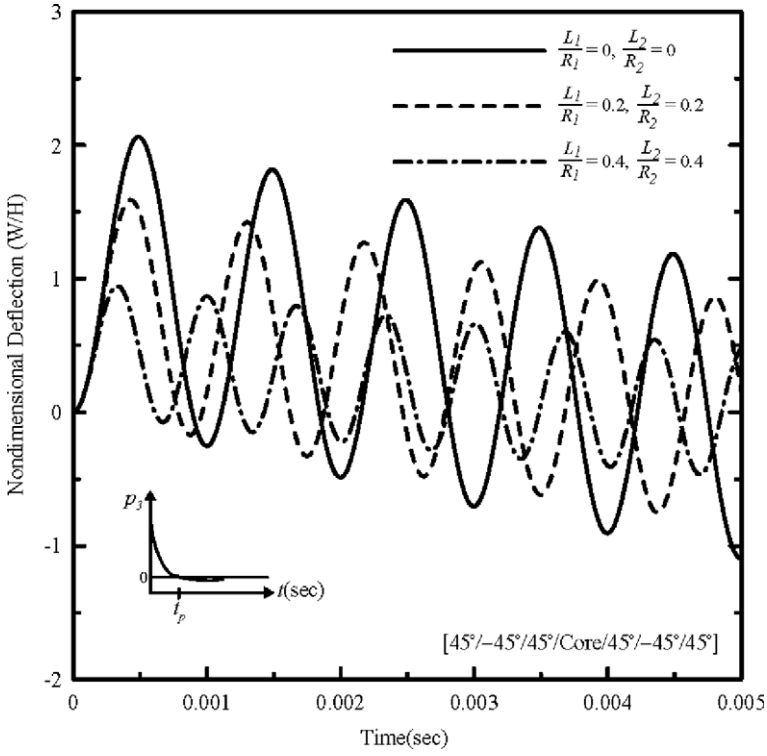

Fig. 15. Influence of the panel curvature on dynamic response to an exponentially decaying pressure pulse ($a/t'_{\mathrm{p}} = 40$).

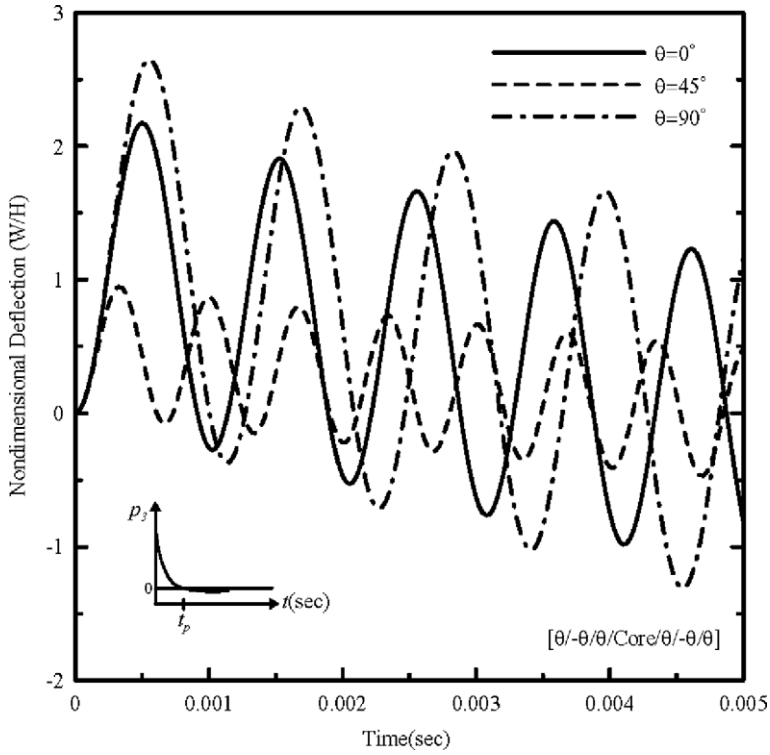

Fig. 16. The counterpart of Fig. 15 for three values of the ply-angle ($a/t'_p = 40$, $L_1/R_1 = L_2/R_2 = 0.4$).

It should also be mentioned that the structural model presented in this paper was validated (see Hause and Librescu, 2006), against the free vibration results available in the literature; obtained via FEM and experimental means, and excellent agreements have been reported.

8. Conclusions

The problem of the dynamic response of doubly-curved anisotropic sandwich panels subjected to various types of blast loadings was addressed. The implications of a number of structural and geometrical characteristics of the sandwich panel, as well as those related to the respective blasts have been highlighted and related conclusions have been drawn.

The beneficial implications of the implementation of the tailoring technique in the face sheets has been emphasized. In this sense, as it has been shown, the structural tailoring applied to sandwich constructions can play an enormous role toward reducing the oscillation amplitudes, and implicitly, toward reducing the danger of the failure by fatigue of the structure. The strong implications of the shell curvature was also put into evidence, in addition to those of other important parameters as damping coefficient, compressive/tensile edge loads, etc.

The adopted solution methodology that is based on the extended Galerkin method considered in conjunction with the Laplace Transform technique enables one to get closed-form solutions of the problem.

The excellent performances of this combined solution methodology have been revealed in various contexts, in the sense of providing accurate solutions (see Librescu and Song, 2005), close to the exact ones.

Appendix A

Strain–displacement relationships in the face sheets and the core layer

Bottom face sheets

$$\varepsilon'_{11} = \xi_{1,1} + \eta_{1,1} - v_3/R_1 \qquad (1 \rightleftarrows 2), \tag{A1a}$$
$$\gamma'_{12} = \xi_{1,2} + \xi_{2,1} + \eta_{1,2} + \eta_{2,1}, \tag{A1b}$$
$$\kappa'_{11} = -v_{3,11} \qquad (1 \rightleftarrows 2), \tag{A1c}$$
$$\kappa'_{12} = -2v_{3,12}. \tag{A1d}$$

Soft core layer

$$\overline{\gamma}_{13} = \frac{1}{\overline{h}}\left\{\eta_1 + \tfrac{1}{2}hv_{3,1}\right\} + v_{3,1} \qquad (1 \rightleftarrows 2), \tag{A2}$$

Top face sheets

$$\varepsilon''_{11} = \xi_{1,1} - \eta_{1,1} - v_3/R_1 \qquad (1 \rightleftarrows 2), \tag{A3a}$$
$$\gamma''_{12} = \xi_{1,2,} + \xi_{2,1} - \eta_{1,2} - \eta_{2,1} \tag{A3b}$$
$$\kappa''_{11} = -v_{3,11} \qquad (1 \rightleftarrows 2), \tag{A3c}$$
$$\kappa''_{12} = -2v_{3,12}. \tag{A3d}$$

Appendix B

Expressions of the global stress-resultants and stress-couples

$$\begin{aligned} &N_{11} = N'_{11} + N''_{11} \qquad (1 \rightleftarrows 2),\\ &N_{12} = N'_{12} + N''_{12},\\ &L_{11} = \overline{h}(N'_{11} - N''_{11}) \qquad (1 \rightleftarrows 2),\\ &L_{12} = \overline{h}(N'_{12} - N''_{12}),\\ &M_{11} = M'_{11} + M''_{11} \qquad (1 \rightleftarrows 2),\\ &M_{12} = M'_{12} + M''_{12}. \end{aligned} \tag{B1a–f}$$

In Eqs. (B1), the stress resultants and stress couples associated with the bottom face sheets are expressed for the shallow shell theory as:

$$\{N'_{\alpha\beta}, M'_{\alpha\beta}\} = \sum_{k=1}^{N} \int_{(x_3)_{k-1}}^{(x_3)_k} (\sigma'_{\alpha\beta})_k \{1, x_3 - a'\}\, \mathrm{d}x_3, \quad (\alpha, \beta = 1, 2) \tag{B2}$$

while the transverse shear stress measures in the core are defined as:

$$\overline{N}_{\alpha 3} = \int_{-\overline{h}}^{\overline{h}} \overline{\sigma}_{\alpha 3}\, \mathrm{d}x_3. \tag{B3}$$

In the above equations, σ_{ij} are the components of the stress tensor.

The stress resultants and stress couples for the upper face can be obtained from Eq. (B2) by replacing single primes by double primes, a' by $-a''$, where, for the present case, $a' = a'' = a$. Herein, N is the number of constituent layers in the bottom face sheets, equal with that in the upper face sheets, while $(x_3)_k$ and $(x_3)_{k-1}$ denote the distances from the global reference plane (coinciding with that of the core layer) to the upper and bottom interfaces of the kth layer, respectively.

Appendix C

2D constitutive equations

Having in view that the top and bottom face sheets are symmetric with respect to both their mid-planes and with the mid-plane of the entire structure, considering that the materials of the face sheets exhibit monoclinic symmetry and that the core material is orthotropic, one obtain the constitutive equations. These equations associated with the bottom face sheets reduced to the mid-plane of the structure are expressed in matrix form as

$$\begin{Bmatrix} N'_{11} \\ N'_{22} \\ N'_{12} \\ M'_{11} \\ M'_{22} \\ M'_{12} \end{Bmatrix} = \begin{bmatrix} A'_{11} & A'_{12} & A'_{16} & E'_{11} & E'_{12} & E'_{16} \\ A'_{21} & A'_{22} & A'_{26} & E'_{21} & E'_{22} & E'_{26} \\ A'_{16} & A'_{26} & A'_{66} & E'_{16} & E'_{26} & E'_{66} \\ E'_{11} & E'_{12} & E'_{16} & F'_{11} & F'_{12} & F'_{16} \\ E'_{21} & E'_{22} & E'_{26} & F'_{21} & F'_{22} & F'_{26} \\ E'_{16} & E'_{26} & E'_{66} & F'_{16} & F'_{26} & F'_{66} \end{bmatrix} \begin{Bmatrix} \varepsilon'_{11} \\ \varepsilon'_{22} \\ \gamma'_{12} \\ \kappa'_{11} \\ \kappa'_{22} \\ \kappa'_{12} \end{Bmatrix}. \tag{C1}$$

The stiffness quantities appearing in Eq. (C1) are defined as

$$\{A'_{\omega\rho}, B'_{\omega\rho}, D'_{\omega\rho}\} = \{A''_{\omega\rho}, B''_{\omega\rho}, D''_{\omega\rho}\} = \sum_{k=1}^{N} \int_{(x_3)_{k-1}}^{(x_3)k} (\hat{Q}'_{\omega\rho})_{(k)}(1, x_3, x_3^2)\,\mathrm{d}x_3 \quad (\omega, \rho = 1, 2, 6), \tag{C2}$$

where $\hat{Q}_{ij} = Q_{ij} - Q_{i3}Q_{j3}/Q_{33}$ denotes the reduced elastic moduli, where for a symmetric construction, $\hat{Q}'_{\omega\rho} = \hat{Q}''_{\omega\rho}$, while

$$E'_{\omega\rho} = B'_{\omega\rho} - a'A'_{\omega\rho} = -E''_{\omega\rho}; \quad F'_{\omega\rho} = D'_{\omega\rho} - 2a'B'_{\omega\rho} + a'^2A'_{\omega\rho} = F''_{\omega\rho} \equiv F_{\omega\rho}. \tag{C3a, b}$$

It should be remarked that for fully symmetric sandwich shells, $E_{\omega\rho} = 0$. The expression of stress resultants and stress couples for the upper face can be obtained from their counterparts associated with the bottom face sheets, by replacing the single prime by double primes.

For the weak core layer considered as an orthotropic body (the axes of orthotropy coinciding with the geometrical axes) the constitutive equations are:

$$\bar{N}_{13} = 2\bar{h}\bar{K}^2\bar{Q}_{55}\bar{\gamma}_{13}, \quad \bar{N}_{23} = 2\bar{h}\bar{K}^2\bar{Q}_{44}\bar{\gamma}_{23}, \tag{C4a, b}$$

where $\bar{K}^2$ is the shear transverse correction factor, while $\overline{Q}_{55}(\equiv \overline{Q}_{13})$ and $\overline{Q}_{44}(\equiv \overline{G}_{23})$ are the transverse shear moduli of the core material.

Appendix D

Expression of the terms appearing in Eqs. (25) and (26).

$(F_1)_{mn}$, $(F_2)_{mn}$, $(G_1)_{mn}$ and $(G_2)_{mn}$ are obtainable as the solution of the matrix equation

$$\begin{bmatrix} (P_{11})_{mn} & (P_{12})_{mn} & (P_{13})_{mn} & (P_{14})_{mn} \\ (P_{12})_{mn} & (P_{11})_{mn} & (P_{14})_{mn} & (P_{13})_{mn} \\ (P_{13})_{mn} & (P_{14})_{mn} & (P_{33})_{mn} & (P_{34})_{mn} \\ (P_{14})_{mn} & (P_{13})_{mn} & (P_{34})_{mn} & (P_{33})_{mn} \end{bmatrix} \begin{Bmatrix} (F_1)_{mn} \\ (F_2)_{mn} \\ (G_1)_{mn} \\ (G_2)_{mn} \end{Bmatrix} = \begin{Bmatrix} (S_1)_{mn} \\ (S_2)_{mn} \\ (S_3)_{mn} \\ (S_4)_{mn} \end{Bmatrix}, \tag{D1}$$

where

$$
\begin{aligned}
(P_{11})_{mn} &= A_{11}m^2 + A_{66}n^2\phi^2,\\
(P_{12})_{mn} &= 2A_{16}mn\phi,\\
(P_{13})_{mn} &= A_{16}m^2 + A_{26}n^2\phi^2,\\
(P_{14})_{mn} &= (A_{12} + A_{66})mn\phi,\\
(P_{33})_{mn} &= A_{22}n^2\phi^2 + A_{66}m^2,\\
(P_{34})_{mn} &= 2A_{26}mn\phi,
\end{aligned}
\tag{D2}
$$

and

$$
\begin{aligned}
(S_1)_{mn} &= -\frac{m}{\pi}(\psi_1 A_{11} + \psi_2\phi A_{12}),\\
(S_2)_{mn} &= -\frac{n\phi}{\pi}(\psi_1 A_{16} + \psi_2\phi A_{26}),\\
(S_3)_{mn} &= -\frac{m}{\pi}(\psi_1 A_{16} + \psi_2\phi A_{26}),\\
(S_4)_{mn} &= -\frac{n\phi}{\pi}(\psi_1 A_{12} + \psi_2\phi A_{22}),
\end{aligned}
\tag{D3}
$$

while $(H_\alpha)_{mn}$ and $(I_\alpha)_{mn}$ are expressed by

$$
(H_1)_{mn} = \frac{a\{[(A_{12} + A_{66})d_2 - A_{22}d_1]\lambda_m\mu_n^2 - d_1A_{66}\lambda_m^3 - d_1d_2\lambda_m\}}{\Delta_{mn}},
\tag{D4}
$$

$$
(I_2)_{mn} = \frac{a\{[(A_{12} + A_{66})d_1 - A_{11}d_2]\lambda_m^2\mu_n - d_2A_{66}\lambda_n^3 - d_1d_2\mu_n\}}{\Delta_{mn}},
\tag{D5}
$$

$$
(H_2)_{mn} = 0, \quad (I_1)_{m,n} = 0,
\tag{D6}
$$

where

$$
\begin{aligned}
\Delta_{mn} = {} & A_{11}A_{66}\lambda_m^4 + (d_2A_{11} + d_1A_{66})\lambda_m^2 + (A_{11}A_{22} - 2A_{12}A_{66} - A_{12}^2)\lambda_m^2\mu_n^2 + (d_1A_{22} + d_2A_{66})\mu_n^2\\
& + A_{22}A_{66}\mu_n^4 + d_1d_2.
\end{aligned}
\tag{D7}
$$

The expression of the operators $\mathcal{L}_{ij}(\bullet)$

$$
\begin{aligned}
&\mathcal{L}_{11}(\bullet) = A_{11}\partial_{11}(\bullet) + 2A_{16}\partial_{12}(\bullet) + A_{66}\partial_{22}(\bullet),\\
&\mathcal{L}_{12}(\bullet)(= \mathcal{L}_{21}(\bullet)) = A_{26}\partial_{22}(\bullet) + A_{16}\partial_{11}(\bullet) + (A_{12} + A_{66})\partial_{12}(\bullet),\\
&\mathcal{L}_{13}(\bullet) = \mathcal{L}_{14}(\bullet)(= \mathcal{L}_{31}(\bullet) = \mathcal{L}_{41}(\bullet)) = 0,\\
&\mathcal{L}_{15}(\bullet)(= \mathcal{L}_{51}(\bullet)) = -(A_{11}/R_1 + A_{12}/R_2)\partial_1(\bullet) - (A_{16}/R_1 + A_{26}/R_2)\partial_2(\bullet),\\
&\mathcal{L}_{22}(\bullet) = A_{22}\partial_{22}(\bullet) + 2A_{26}\partial_{12}(\bullet) + A_{66}\partial_{11}(\bullet),\\
&\mathcal{L}_{23}(\bullet) = \mathcal{L}_{24}(\bullet)(= \mathcal{L}_{32}(\bullet) = \mathcal{L}_{42}(\bullet)) = 0,\\
&\mathcal{L}_{25}(\bullet)(= \mathcal{L}_{52}(\bullet)) = -(A_{22}/R_2 + A_{12}/R_1)\partial_2(\bullet) - (A_{26}/R_2 + A_{16}/R_1)\partial_1(\bullet),\\
&\mathcal{L}_{33}(\bullet) = A_{11}\partial_{11}(\bullet) + A_{66}\partial_{22}(\bullet) + 2A_{16}\partial_{12}(\bullet) - d_1,\\
&\mathcal{L}_{34}(\bullet)(= \mathcal{L}_{43}(\bullet)) = (A_{12} + A_{66})\partial_{12}(\bullet) + A_{16}\partial_{11}(\bullet) + A_{26}\partial_{22}(\bullet),\\
&\mathcal{L}_{35}(\bullet) = (\mathcal{L}_{53}(\bullet)) = -d_1a\partial_1(\bullet),\\
&\mathcal{L}_{44}(\bullet) = A_{22}\partial_{22}(\bullet) + A_{66}\partial_{11}(\bullet) + 2A_{26}\partial_{12}(\bullet) - d_2,\\
&\mathcal{L}_{45}(\bullet)(= \mathcal{L}_{54}(\bullet)) = -d_2a\partial_2(\bullet),\\
&\mathcal{L}_{55}(\bullet) = (A_{11}/R_1^2 + A_{22}/R_2^2 + 2A_{12}/R_1R_2) - d_1a^2\partial_{11}(\bullet) - d_2a^2\partial_{22}(\bullet) + F_{11}\partial_{1111}(\bullet)\\
&\qquad + F_{22}\partial_{2222}(\bullet) + 4F_{66}\partial_{1122}(\bullet) + 2F_{12}\partial_{1122}(\bullet) + 4F_{16}\partial_{1112}(\bullet) + 4F_{26}\partial_{1222}(\bullet)\\
&\qquad + N_{11}^0\partial_{11}(\bullet) + N_{22}^0\partial_{22}(\bullet) + C\partial_t(\bullet) + m_0\partial_{tt}(\bullet),
\end{aligned}
\tag{D8a–l}
$$

where the usual differentiation symbols, $\partial_{ij}(\bullet) \equiv \partial^2(\bullet)/\partial x_i\partial x_j$, and $\partial_{tt}(\bullet) \equiv \partial^2(\bullet)/\partial t^2$ have been used.

Appendix E

Expression of undamped natural frequencies ω_{mn}^2

$$\omega_{mn}^2\left[=\frac{\pi^4 F_{11}}{m_0 L_1^4}\right] = m^4 + \frac{F_{22}n^4\phi^4}{F_{11}} + \frac{2(F_{12}+2F_{66})m^2n^2\phi^2}{F_{11}} + \frac{a^2L_1^2}{F_{11}\pi^2}(d_1m^2 + d_2^2n^2\phi^2)$$
$$+ \frac{aL_1^3}{F_{11}\pi^3}(d_1m(H_1)_{mn} + d_2n\phi(I_2)_{mn} + \frac{L_1^2}{F_{11}\pi^3}[m(\psi_1A_{11}+\psi_2\phi A_{12})(\tilde{F}_1)_{mn}$$
$$+ n\phi(\psi_1A_{12}+\psi_2\phi A_{22})(G_2)_{mn} + (n\phi(F_2)_{mn} + m(G_1)_{mn})(\psi_1A_{16}+\phi\psi_2A_{26})]$$
$$+ \frac{L_1^2}{F_{11}\pi^4}(\psi_1^2A_{11} + \psi_2^2\phi^2A_{22} + 2A_{12}\psi_1\psi_2\phi) - K_x(m^2\psi^2 + L_Rn^2\psi^2\phi^2). \tag{E1}$$

Herein $\psi_1 = L_1/R_1$; $\psi_2 = L_2/R_2$; $\phi = L_1/L_2$; $K_x = L_1^2N_{11}^0/\pi^4F_{11}$; $L_R = N_{22}^0/N_{11}^0$, while the expressions of $(H_1)_{mn}$, $(I_2)_{mn}$, $(F_\alpha)_{mn}$ and $(G_\alpha)_{mn}$ are supplied in Appendix D.

Appendix F

The expressions of $q_{mn}(t)$ *for various pressure pulses*

For a *step pulse* as provided by Eq. (18b):

$$q_{mn}(t) = \frac{\tilde{F}_{mn}}{m_0\omega_{mn}^2}\left\{1 - e^{-\Delta_{mn}\omega_{mn}t}\cos\Omega_{mn}t - \frac{\Delta_{mn}}{\sqrt{1-\Delta_{mn}^2}}e^{-\Delta_{mn}\omega_{mn}t}\sin\Omega_{mn}t\right\}, \tag{F1}$$

where here and in the next equations,

$$\Omega_{mn} = \omega_{mn}\sqrt{1-\Delta_{mn}^2}, \tag{F2}$$

and

$$\tilde{F}_{mn} = \frac{16P_0\delta_{m,2s-1}\delta_{n,2q-1}}{\pi^2(2s-1)(2q-1)} \quad (s,q=1,2,\ldots), \tag{F3}$$

where $\delta_{m,2s-1}$ was defined by (26b).

For a *rectangular pressure pulse*, (Eq. (18a)):

$$q_{mn} = \frac{\tilde{F}_{mn}}{m_0\omega_{mn}^2}\left\{1 - e^{-\Delta_{mn}\omega_{mn}t}\cos\Omega_{mn}t - \frac{\Delta_{mn}}{\sqrt{1-\Delta_{mn}^2}}e^{-\Delta_{mn}\omega_{mn}t}\sin\Omega_{mn}t\right.$$
$$\left. - \left[1 - e^{-\Delta_{mn}\omega_{mn}(t-t_p)}\cos\Omega_{mn}(t-t_p) - \frac{\Delta_{mn}}{\sqrt{1-\Delta_{mn}^2}}e^{-\Delta_{mn}\omega_{mn}(t-t_p)}\sin\Omega_{mn}(t-t_p)\right]H(t-t_p)\right\}. \tag{F4}$$

For a N-shaped pulse, Eq. (17):

$$q_{mn}(t) = \frac{\tilde{F}_{mn}}{m_0\omega_{mn}^2}\left\{1 + 2\frac{\Delta_{mn}}{t_p\omega_{mn}} - \frac{t}{t_p} - \left(1 + \frac{2\Delta_{mn}}{t_p\omega_{mn}}\right)e^{-\Delta_{mn}\omega_{mn}t}\cos\Omega_{mn}t\right.$$
$$- \left(\frac{2\Delta_{mn}^2 + \Delta_{mn}\omega_{mn}t_p - 1}{\Omega_{mn}t_p}\right)e^{-\Delta_{mn}\omega_{mn}t}\sin\Omega_{mn}t$$
$$- \left[1 + \frac{2\Delta_{mn}}{t_p\omega_{mn}} - \frac{t}{t_p} - \left\{(1-r) + \frac{2\Delta_{mn}}{t_p\omega_{mn}}\right\}e^{-\Delta_{mn}\omega_{mn}(t-rt_p)}\cos\Omega_{mn}(t-rt_p)\right.$$
$$\left.\left. - \left(\frac{2\Delta_{mn}^2 + (1-r)t_p\omega_{mn}\Delta_{mn} - 1}{\Omega_{mn}t_p}\right)e^{-\Delta_{mn}\omega_{mn}(t-rt_p)}\sin\Omega_{mn}(t-rt_p)\right]H(t-rt_p)\right\}. \tag{F5}$$

For a *sine-pulse* (Eq. 19):

$$q_{mn}(t) = \frac{\tilde{F}_{mn}\pi}{m_0 t_p}\Big\{(a_1)_{mn}\cos(\pi t/t_p) + (b_1)_{mn}\frac{t_p}{\pi}\sin(\pi t/t_p) + (a_2)_{mn}e^{-\Delta_{mn}\omega_{mn}t}\cos\Omega_{mn}t + \left(\frac{(b_2)_{mn} - (a_2)_{mn}\Delta_{mn}\omega_{mn}}{\Omega_{mn}}\right)e^{-\Delta_{mn}\omega_{mn}t}\sin\Omega_{mn}t + [(a_1)_{mn}\cos\pi(t-t_p)/t_p + \frac{(b_1)_{mn}t_p}{\pi}\sin\pi(t-t_p)/t_p + (a_2)_{mn}e^{-\Delta_{mn}\omega_{mn}(t-t_p)}\cos\Omega_{mn}(t-t_p) + \frac{\left((b_2)_{mn} - (a_2)_{mn}\Delta_{mn}\omega_{mn}\right)}{\Omega_{mn}}e^{-\Delta_{mn}\omega_{mn}(t-t_p)}\sin\Omega_m(t-t_p)]H(t-t_p)\Big\}, \tag{F6a}$$

where coefficients $(a_\alpha)_{mn}$ and $(b_\alpha)_{mn}$ are as follows:

$$(a_1)_{mn} = -(a_2)_{mn} = \frac{2t_p^2\Delta_{mn}\omega_{mn}^2}{\pi^2}\left\{[\omega_{mn}^2 - \pi^2/t_p^2]\left(1 - \frac{\omega_{mn}^2 t_p^2}{\pi^2}\right) - 4\Delta_{mn}^2\omega_{mn}^2\right\}^{-1},$$

$$(b_1)_{mn} = \frac{1 - \omega_{mn}^2 t_p^2/\pi^2}{\omega_{mn}^2 - \pi^2/t_p^2)\left(1 - \frac{\omega_{mn}^2 t_p^2}{\pi^2}\right) - 4\Delta_{mn}^2\omega_{mn}^2}, \tag{F6b–d}$$

$$(b_2)_{mn} = -[(1 - \omega_{mn}^2 t_p^2/\pi^2) - 4\Delta_{mn}^2\omega_{mn}^2 t_p^2/\pi^2\left\{(\omega_{mn}^2 - \pi^2/t_p^2)\left(1 - \frac{\omega_{mn}^2 t_p^2}{\pi^2}\right) - 4\Delta_{mn}^2\omega_{mn}^2\right\}^{-1}.$$

Finally, corresponding to a *shock-wave traveling* along the x_1-direction (Eq. (20)) the solution for q_{mn} is

$$q_{mn}(t) = \frac{\tilde{F}_{mn}}{m_0}\Big\{Ae^{-\eta c(t-x_1/c)} + B[e^{-\Delta_{mn}\omega_{mn}(t-x_1/c)}\cos\Omega_{mn}t - \frac{1}{\Omega_{mn}}e^{-\Delta_{mn}\omega_{mn}(t-x_1/c)}\Delta_{mn}\omega_{mn}\sin\Omega_{mn}(t-x_1/c)] + \frac{c}{\Omega_{mn}}e^{-\Delta_{mn}\omega_{mn}(t-x_1/c)}\sin\Omega_{mn}(t-x_1/c)\Big\}H(t-x_1/c), \tag{F7a}$$

where

$$A = -B = [\omega_{mn}^2 + \eta c(\eta c - 2\Delta_{mn}\omega_{mn})]^{-1}, \tag{F7b, c}$$

$$C = \frac{\eta c - 2\Delta_{mn}\omega_{mn}}{\omega_{mn}^2 + \eta c(\eta c - 2\Delta_{mn}\omega_{mn}^2)}.$$

As a general comment, the expressions of q_{mn} have been derived by including the damping effect. The undamped counterpart of q_{mn}, and implicitly, of the dynamic response can be obtained by letting in Eqs. (F1)–(F7), $\Delta_{mn} \to 0$.

References

Abrate, S., 1997. Localized impact on sandwich structures with laminated facings. Applied Mechanical Review 50, 69–82.

Birman, V., Bert, C.W., 1987. Behavior of laminated plates subjected to conventional blast. Journal of Impact Engineering 6 (3), 145–155.

Cederbaum, G., Librescu, L., Elishakoff, I., 1988. Dynamic response of flat panels made of advanced composite materials subjected to random excitation. The Journal of the Acoustical Society of America 84 (2), 660–666.

Cederbaum, G., Librescu, L., Elishakoff, I., 1989. Response of laminated plates to no-stationary random excitation. Structural Safety 6, 99–113.

Crocker, M.J., Hudson, R.R., 1969. Structural response to sonic boom. Journal of Sound and Vibration 9 (3), 454–468.

Dobyns, A.L., 1981. Analysis of simply-supported orthotropic plates subjected to static and dynamic loads. AIAA Journal 19, 642–650.

Frostig, Y., 2003. Classical and high-order computational models in the analysis of modern sandwich panels. Composites Part B Engineering 34, 83–100.

Gol'denveiser, A.L., 1961. Theory of Elastic Thin Shells. Pergameon Press, Oxford, London, New York, Paris.

Hause, T., Librescu, L., Camarda, C.J., 1998. Postbuckling of anisotropy flat and doubly-curved panels under complex loading conditions. International Journal of Solids and Structures 35, 3007–3038.

Hause, T., Johnson, T.F., Librescu, L., 2000. Effect of face-sheet anisotropy on buckling and post-buckling of flat sandwich panels. Journal of Spacecraft and Rockets 37 (3), 331–341.

Hause, T., Librescu, L., 2005. Dynamic response of anisotropic sandwich flat panels to explosive pressure pulses. International Journal of Impact Engineering 31 (5), 607–628.
Hause, T., Librescu, L., 2006. Flexural free vibration of sandwich flat panels with laminated anisotropic face sheets. Journal of Sound and Vibration 297 (3–5), 823–841.
Hohe, J., Librescu, L., 2004. Advances in the structural modeling and behavior of sandwich panels. Mechanics of Advanced Materials and Structures 11 (4–5), 395–424.
Hohe, J., Librescu, L., Oh, S.-Y., 2006. Dynamic buckling of flat and curved sandwich panel with transversely compressible core. Composite Structures 74 (1), 10–24.
Leissa, A.W., 1973. Vibration of Shells, NASA-SP-288, NASA, Washington DC, pp. 32–33.
Kim, D.-H., Han, J.-H., 2006. Establishment of gun blast wave model and structural analysis for blast load. Journal of Aircraft 43 (4), 1159–1168.
Librescu, L., 1975. Elastostatics and Kinetics of Anisotropic and Heterogeneous Shell-type Structures. Noordhoff International Publishing, Leyden, Netherlands.
Librescu, L., Nosier, A., 1990. Response of shear deformable elastic laminated composite panels to sonic boom and explosive blast loadings. AIAA Journal 28 (2), 345–352.
Librescu, L., Hause, T., Camarda, C.J., 1997. Geometrically nonlinear theory of initially imperfect sandwich plates and shells incorporating non-classical effects. AIAA Journal 35 (8), 1393–1403.
Librescu, L., Hause, T., 2000. Recent developments in the modeling and behavior of advanced sandwich constructions: a survey. Journal of Composite Structures 48 (1–3), 1–17.
Librescu, L., Oh, S.-Y., Hohe, J., 2004. Linear and non-linear dynamic response of sandwich panels to blast loading. In: Rajapakse, Y., Hui, D. (Eds.), Composites B, Special Issue on Marine Composites 35, Elsevier, 6–8, September, pp. 673–683.
Librescu, L., Song, O., 2005. Thin-walled Composite Beams: Theory and Application. Springer, Netherlands.
Librescu, L., Oh, S.-Y., Hohe, J., 2006. Dynamic response of anisotropic sandwich flat panels to underwater and in-air explosions. International Journal of Solids and Structures 43 (13), 3794–3816.
Marzocca, P., Librescu, L., Chiocchia, G., 2001. Aeroelastic response of 2-D lifting surfaces to gust and arbitrary explosive loading signature. International Journal of Impact Engineering 25 (1), 67–85.
Noor, A.K., Burton, W.S., Bert, C.W., 1996. Computational models for sandwich plates and shells. Applied Mechanics Reviews 49, 155–199.
Qatu, M.S., 2004. Vibration of Laminated Shells and Plates. Elsevier Acad. Press, pp. 196–197.
Rajamani, A., Prabhakaran, R., 1980. Response of composite plates to blast loading. Experimental Mechanics 20, 245–250.
Reddy, J.N., 2004. Mechanics of Laminated Composite Plate and Shells: Theory and Analysis, second ed. CRC Press, NY, USA.
Thomsen, O.T., Bozhevolnaya, E., Lychegaard, A. (Eds.), 2005. Advancing with Sandwich Structures and Materials, Proceedings of the International Conference on Sandwich Structures. Springer.
Vinson, J.R., 1991. The Behavior of Sandwich Structures of Isotropic and Composite Materials. Technomic Publ., Lancaster, PA.
Vinson, J.R., 2001. Sandwich Structures. Applied Mechanics Reviews 54, 201–214.
Vinson, J.R., Rajapakse, Y.D.S., Carlsson, L.E. (Eds.), 2003. Sixth International Conference on Sandwich Structures. CRC Press, Boca Raton, London, New York, Washington, DC.
Vu-Quoc, L., Ebcioglu, I.K., Deng, H., 1997. Dynamic formulation for geometrically-exact sandwich shells. International Journal of Solids and structures 34 (20), 2517–2548.
Vu-Quoc, L., Deng, H., Tan, X.G., 2001. Geometrically-exact sandwich shells: the dynamic case. Computer Methods in Applied Mechanics and Engineering 190 (22–23), 2825–2873.
Xue, Z., Hutchinson, J.W., 2004. A comparative study of impulse-resistant metal sandwich plates. International Journal of Impact Engineering 30, 1283–1305.
Zenkert, D., 1995. An Introduction to Sandwich Construction. EMAS Publ., Chameleon Press LTD, London, UK.